Supplementary Materials: Safety Issues of Defected Lithium-ion Batteries: Identification and Risk Evaluation

Yikai Jia[1, 2], Binghe Liu[3, 4], Zhiguo Hong[3, 4], Sha Yin[3, 4], Donal P. Finegan[5], Jun Xu[1, 2*]

[1] *Department of Mechanical Engineering and Engineering Science, The University of North Carolina at Charlotte, Charlotte, NC 28223, USA*

[2] *Vehicle Energy & Safety Laboratory (VESL), North Carolina Motorsports and Automotive Research Center, The University of North Carolina at Charlotte, Charlotte, NC 28223, USA*

[3] *Department of Automotive Engineering, School of Transportation Science and Engineering, Beihang University, Beijing 100191, China*

[4] *Vehicle Energy & Safety Laboratory (VESL), Beihang University, Beijing 100191, China*

[5] *National Renewable Energy Laboratory, 15013 Denver West Parkway, Golden CO 80401, USA*

[*] Corresponding author: Dr. Jun Xu at jun.xu@uncc.edu; Tel: (704)-687-8240; Fax: (704)-687-8240

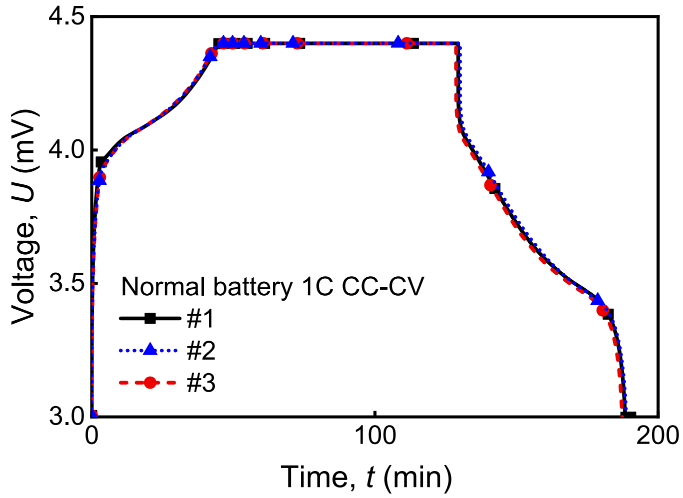

Fig. S1 1C CC-CV voltage-time curve for cell used during the screw indentation.
(Section 2: Manufacture of defective battery)

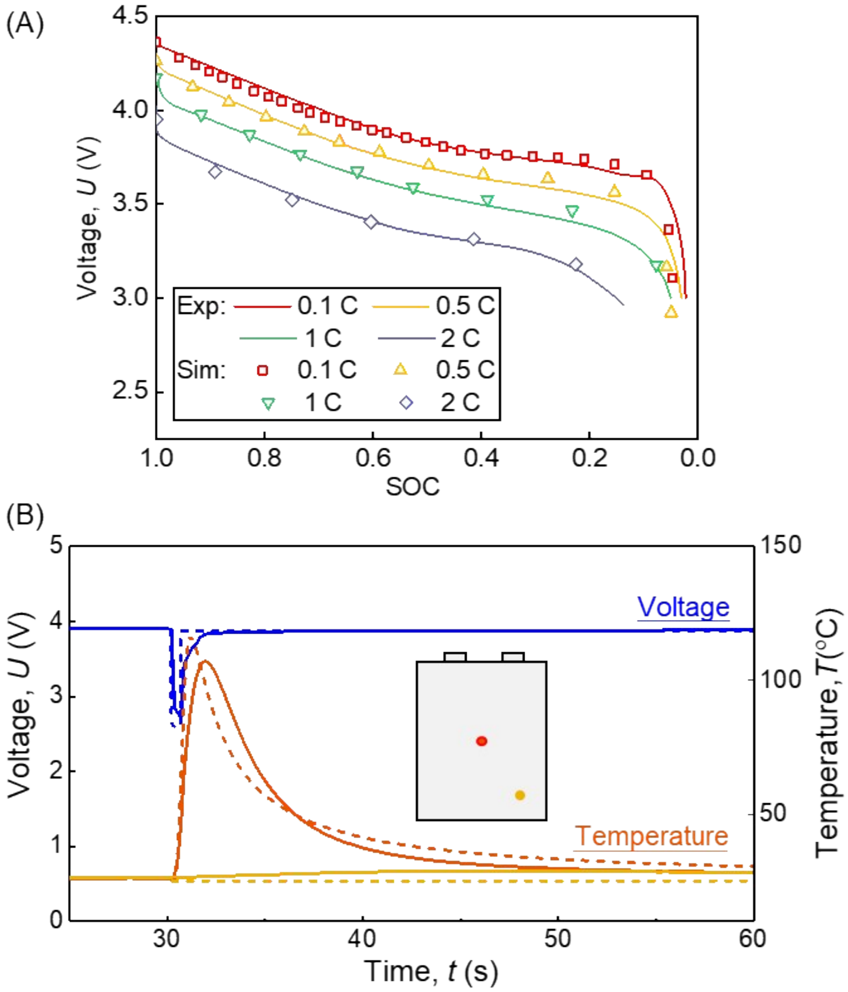

Fig. S2 Validations of the submodels within the multiphysics coupling model. A) Battery model. Comparison of discharging voltage curves at different rates between simulation and experiment; B) Electrochemical-thermal coupling model. Comparison of voltage, temperature curve after the onset of the ISC during the screw penetration loading. Section 2: Electro-chemo-thermal coupling model)

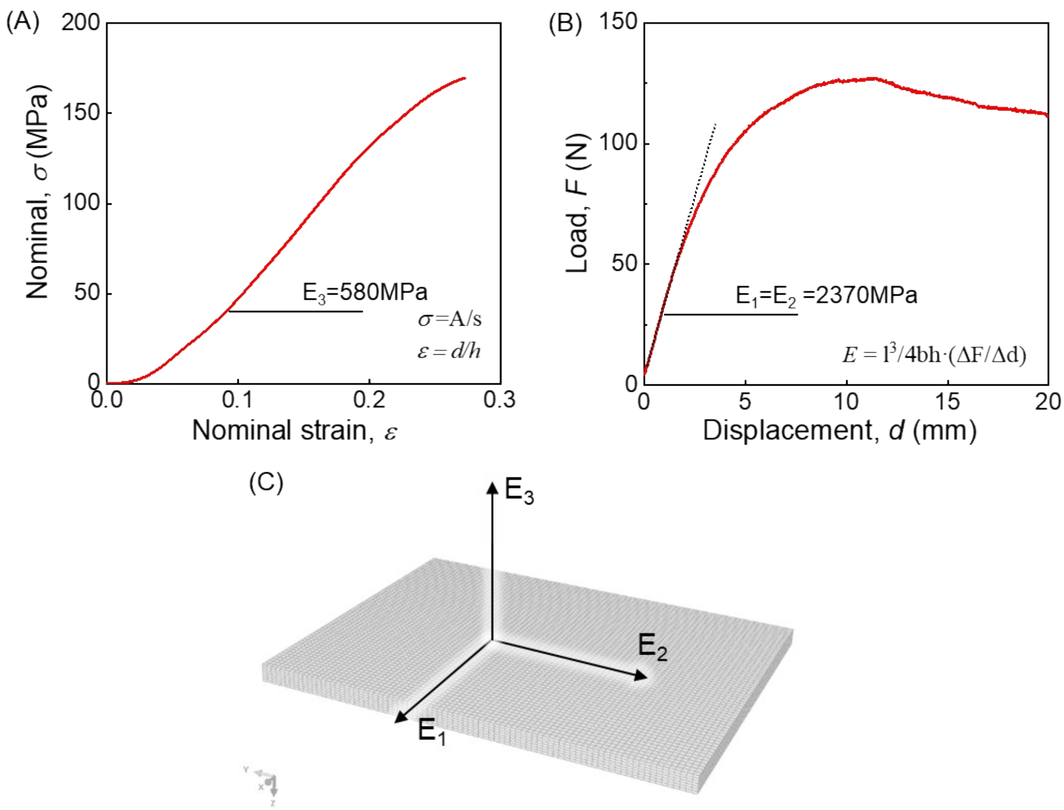

Fig. S3 Material properties for the battery model. The model used here is an anisotropic elastoplastic homogenous model. A) Constitutive relationship obtained by out-of-plane compression test; B) In-plane elastic modulus estimated by three-point bending; C) Material coordinate system definition. (Section 2: Mechanical test for safety evaluation)

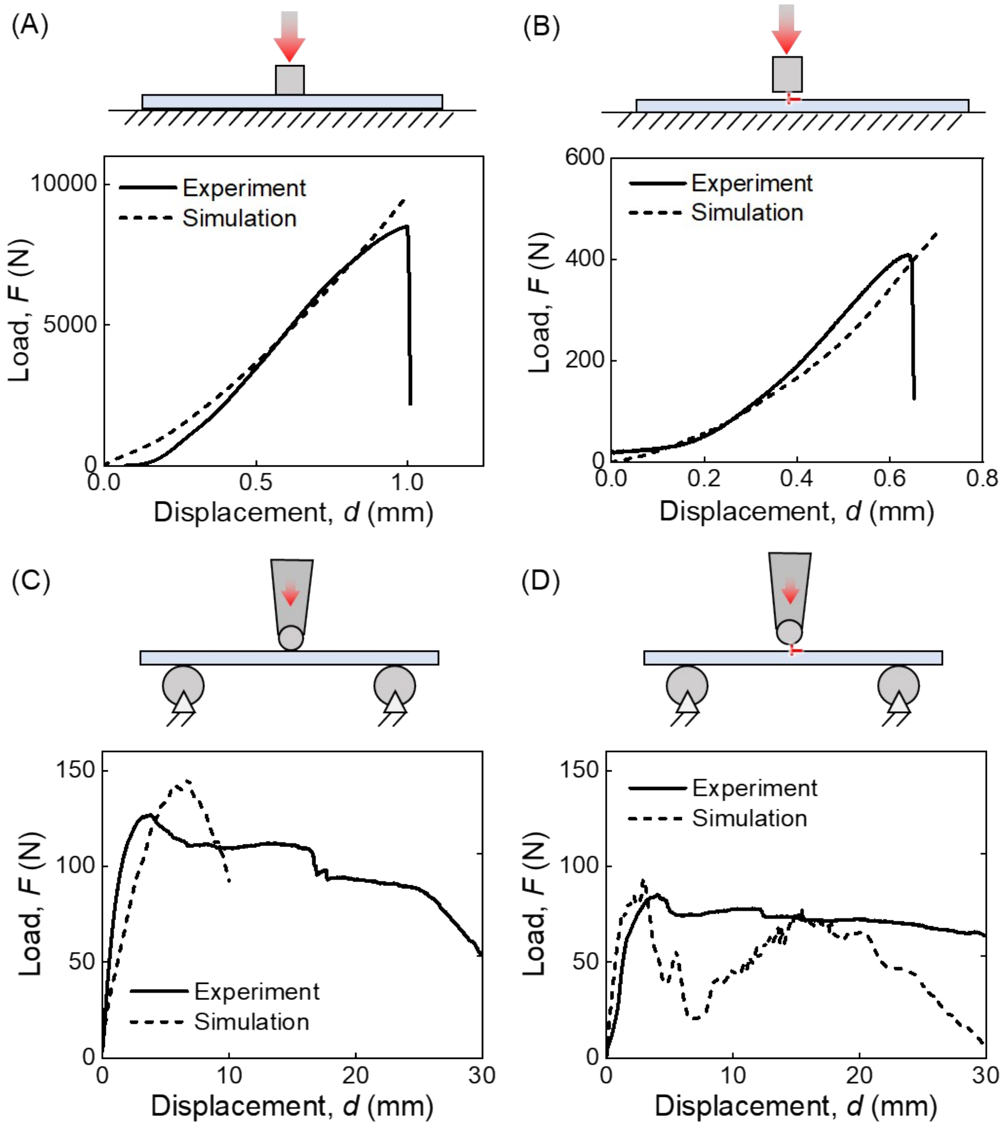

Fig. S4 Validation of the finite element model. A) normal battery indentation; B) defected battery indentation. C) normal battery 3-point bending. D) defected battery 3-point bending. (Section 2: Mechanical test for safety evaluation)

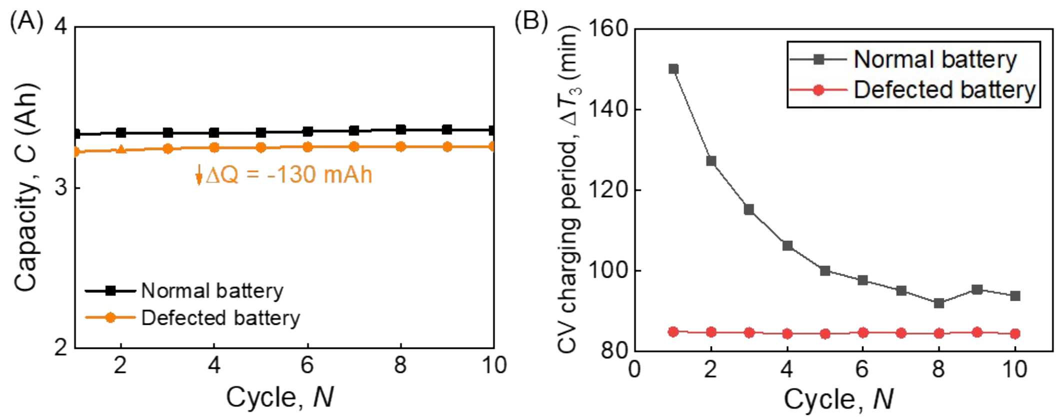

Fig. S5 Changes in electrochemical characteristics of the defected battery. A) comparison of 1C CC-CV cycling capacity curves between the defected battery and the normal battery; B) Comparison of CV stage period-cycle curve (Section 3: Characterization of defected batteries).

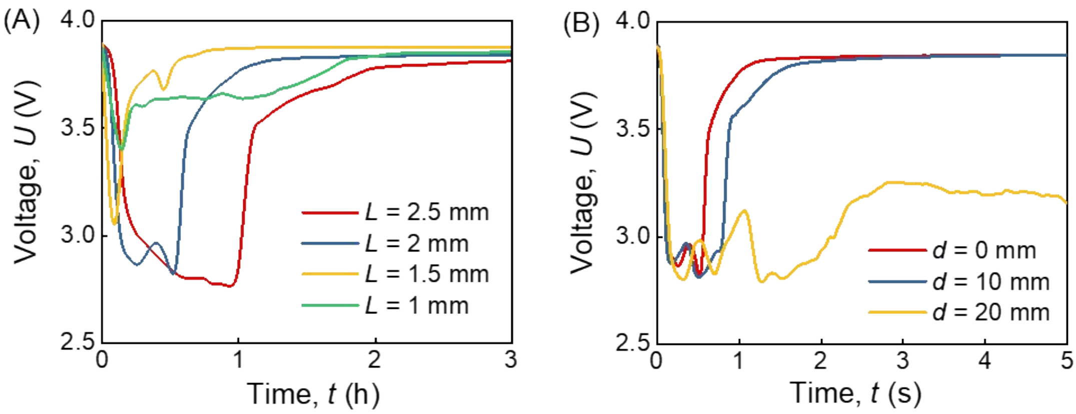

Fig. S6 Effect of indenter sizes and indentation positions (1C CC cycling, sphere steel particle). (A) voltage response at different indenter size (from 1.0 mm to 2.5 mm diameter, center); (B) voltage response at different positions (0, 10, 20 mm from center, 2 mm). (Section 3: Effect of defect at different sizes and positions)

Calculation of steady-state temperature

(Section 4: Electrochemical-thermal safety evaluation of defective battery)

The steady-state temperature can be estimated theoretically based on the defected battery equivalent circuit and thermal dynamic equation as

$$\rho V C_{\mathrm{p}} \frac{\mathrm{d}T}{\mathrm{d}t} = \dot{Q}_{\mathrm{j}} + \dot{Q}_{\mathrm{h}} + \dot{Q}_{\mathrm{r}}, \tag{1}$$

where C_p is the specific thermal capacity of the battery, ρ is the density of the battery, V is the volume of the battery, T is the battery temperature, $\dot{Q}_j$ is the joule heat power, $\dot{Q}_h$ is the thermal convection power, and $\dot{Q}_r$ is the thermal radiation power. According to Ohm's law,

$$I_s = \frac{E}{R_s + R_0}, \tag{2}$$

where I_s is the short-circuit current (current leakage), R_s is the short-circuit resistance, R_0 is the internal resistance and E is the potential of the cell. The charging current I_d is equal to the sum of short-circuit current and current through the electrodes I_0:

$$I_d = I_s + I_0, \tag{3}$$

According to Joule's law,

$$\dot{Q}_J = I_s^2 (R_s + R_0), \tag{4}$$

The thermal convection power is

$$\dot{Q}_h = (T - T_{amb}) hA, \tag{5}$$

where T_{amb} is the ambient temperature, h is the air convection coefficient and A is the convection area. The thermal radiation power is

$$\dot{Q}_r = (T^4 - T_{amb}{}^4)\sigma \varepsilon A, \tag{6}$$

where σ is the surface emissivity and ε is the Stefan-Boltzmann constant.

For steady-state condition,

$$\frac{\mathrm{d}T}{\mathrm{d}t} = 0, \tag{7}$$

Solving the equations we can obtain $T = T_s$.

Table S1 Values used in the equations for chemical reaction and phase change (Table 2).

Parameters	Value
$A_{\text{c-e}}$	6.667×10^{13} (1/s)
A_{e}	5.14×10^{25} (1/s)
A_{sei}	1.667×10^{15} (1/s)
$A_{\text{a-e}}$	2.5×10^{13} (1/s)
A_{sep}	2.5×10^{28} (1/s)
A_{cc}	2.5×10^{30} (1/s)
c_{sei0}	0.15
α_{c-e0}	0.04
c_{a0}	0.75
c_{e0}	1
c_{sep0}	1
c_{cc0}	1
z_0	0.033
$E_{\text{a-e}}$	1.35×10^{5} (J/mol)
$E_{\text{c-e}}$	1.39×10^{5} (J/mol)
E_{sei}	1.35×10^{5} (J/mol)
E_{e}	2.74×10^{5} (J/mol)
$E_{\text{cc\_cu}}$	7.2×10^{5} (J/mol)
$E_{\text{cc\_al}}$	5.1×10^{5} (J/mol)
E_{sep}	2.5×10^{5} (J/mol)
$H_{\text{a-e}}$	1714 (J/g)
$H_{\text{c-e}}$	400 (J/g)
H_{sei}	257 (J/g)
H_{e}	155 (J/g)
W_{c}	610.4 (kg/m^3)
W_{p}	1221000 (kg/m^3)
W_{e}	406.9 (kg/m^3)